Kinetic effects in recombination of optical excitations in disordered quantum heterostructures: Theory and experiment

O. Rubel*, S.D. Baranovskii, K. Hantke, B. Kunert, W.W. Rühle,
P. Thomas, K. Volz, W. Stolz

Faculty of Physics and Material Sciences Center, Philipps-Universität Marburg, Marburg 35032, Germany

Abstract

An overview of recent experimental and theoretical results on stationary and time-dependent photoluminescence spectra in disordered semiconductor heterostructures is presented. In particular, temperature-dependent peak position and linewidth of the luminescence spectra, as well as the luminescence intensity are considered along with the time evolution of the luminescence intensity after pulsed excitation. Emphasis is given on the comparison between experimental and theoretical results aiming at a characterization of disorder in the underlying structures.

Contents

1. Introduction

Semiconductor III–V heterostructures alloyed with nitrogen inevitably possess a certain degree of disorder due to their alloy structure and/or imperfect interfaces [1]. The disorder of potential energy gives rise to carrier

*Corresponding author. Tel.: +49 6421 2824241;
fax: +49 6421 2828935.

E-mail address: Oleg.Rubel@Physik.Uni-Marburg.de (O. Rubel).

localization, in particular at low temperatures, that dramatically affects optical properties of dilute nitride semiconductors [2–4]. Measurements of the photoluminescence (PL) response has become a routine tool for characterizing the quality of the samples, in particular for revealing the energy scale of the disorder potential. The PL peak energy and the PL linewidth in dilute nitride heterostructures demonstrate nonmonotonic temperature dependences [1,3,5,6]. The most prominent experimental observations are: (i) an anomalous red shift of the PL peak

energy in the range of intermediate temperatures, the so-called S-shape behavior; (ii) broadening of the PL line-width within a narrow temperature range; (iii) a decrease of the integrated PL intensity by orders of magnitude with increasing temperature. These features of the PL spectra suggest an essential role of disorder in the dynamics of recombining excitations [2,7–11]. However, the extraction of disorder parameters from experimental temperature-dependent PL spectra is not straightforward and requires a theoretical basis.

The experimentally observed effects of disorder on the dynamics of recombining carriers can be reproduced within a model where spatially localized excitons hop between localized states distributed randomly in space and energy [11]. This model was successfully applied to the explanation of the temperature dependences of PL spectra in (GaIn)(NAs)/Ga(N)As quantum wells (QWs) [12,13], (ZnCd)Se quantum islands [14], and (InGa)N/GaN QWs [15]. Recently this model was extended in order to account for nonradiative processes responsible for quenching of the PL with increasing temperature [16].

In this paper we present an overview of recent achievements in experimental and theoretical studies of temperature- and time-dependent PL spectra in dilute nitride semiconductors. We show that it is possible to achieve quantitative estimates for the parameters characterizing the disorder. In particular, a comparison between experimental spectra and theoretical calculations provides a direct access to the energy spectrum of potential fluctuations, to the density of localized states, and that of nonradiative centers.

2. Temperature dependence of the PL spectra

At low temperatures, the PL spectrum of dilute nitride semiconductors is governed by the recombination of excitations trapped by local fluctuations of the band edges [2]. The origin of these fluctuations is traditionally associated with compositional inhomogeneities and nitrogen complexes that form shallow localized states and produce extended band tails [17]. A comprehensive analysis of temperature-dependent PL data for (GaIn)(NAs) QWs showed that the band tail has an exponential form [12,13]

$$g(E) = \frac{N_0}{E_0} \exp\left(\frac{E}{E_0}\right), \tag{1}$$

with a characteristic energy scale E_0 and a concentration of localized states N_0. (The origin of the energy scale in Eq. (1) is set to the mobility edge.) It is also known that nitrogen primarily affects the conduction band edge, while the valence band remains almost unperturbed [18]. Therefore, photoexcited electrons become readily localized, while the photoexcited holes remain mobile and can form spatially correlated pairs (excitons) due to their Coulomb interaction with electrons. The problem is thus reduced to the case of strongly correlated electron–hole pairs in the

form of excitons, assuming that such pairs can be localized with respect to their center-of-mass coordinate [19].

Excitons trapped in localized states perform phonon-assisted hopping transitions between localized states in the band tail. The transition rate between two localized states depends exponentially on the spatial separation between sites and on the difference in energy between them [20]. Excitons perform their hopping dynamics until the inverse hopping rate becomes comparable to the radiative lifetime τ_0. The PL spectrum is determined by the energy distribution of excitons, which is a function of time and temperature. Despite the transparency of the physical picture, its exact analytical solution remains a challenge so far. An efficient way to calculate the temperature-dependent PL spectra is to perform kinetic Monte Carlo simulations of hopping and recombination of excitons in the manifold of localized states [11].

At low temperatures, excitons hop predominantly downward in energy losing (in average) the energy of E_0 in every hopping event. An exciton performs several hops within its lifetime (a few nanoseconds), that gives rise to an appreciable Stokes shift[1] of the PL spectra, $E_{st} \approx (2.5 - 4.5)E_0$ at $T \to 0$. When temperature increases, excitons become more mobile, and the PL emission energy shifts to lower energies with respect to its position at $T = 0$. The absolute value of the Stokes shift achieves its maximum at temperature $T_{tr} \approx 0.7E_0/k_B$ [11–14], where k_B is Boltzmann's constant. At higher temperatures, the exciton distribution approaches thermal equilibrium, and the PL energy readily shifts towards the mobility edge. The establishment of thermal equilibrium is accompanied by an abrupt increase and subsequent decrease of the PL linewidth. Such broadening results from the interplay between the exponential density of localized states (DOS) and the Boltzmann population function, and it is evidence for the exponential shape of the DOS in the band tail [12–14]. The broadening achieves its maximum at temperature $T_2 \approx E_0/k_B$. This is the transient temperature at which the energy relaxation mechanism changes from energy-loss hopping to the regime similar to multiple-trapping. A comprehensive description of the simulation algorithm and of the theoretical results can be found elsewhere [11–14].

Now we would like to illustrate the theory by its application to the experimental data. The temperature dependences of the PL peak-energy position and of the PL linewidth measured for as-grown, annealed, and hydrogenated (GaIn)(NAs) samples are shown in Fig. 1. These data exhibit the main features inherent in temperature-dependent PL properties of disordered semiconductors.

Before we proceed with the quantitative analysis of the experimental data, we shall verify the shape of the DOS in the band tail. All three samples clearly show a peak in their

---

[1] While interpreting the simulation results, we define the Stokes shift as a difference between the PL peak energy and origin of the energy scale in Eq. (1), which corresponds to the exciton mobility edge.

temperature dependence of the PL linewidth (FWHM) in Fig. 1(b). This feature clearly provides evidence for the exponential shape of the DOS [12–14]. Next we can determine the DOS energy scale E_0 in Eq. (1). All three samples demonstrate a nonmonotonic temperature dependence of the PL peak energy [Fig. 1(a)]. The transient temperatures T_{tr}, which correspond to maximum value of the Stokes shift, are for all samples about $T_{tr} \approx 40\,\text{K}$ suggesting $E_0 \approx 0.7 T_{tr}/k_B = 5\,\text{meV}$. However, this value of E_0 is only a rough estimate, since it is difficult to locate T_{tr} precisely, particularly in the case of a hydrogenated sample. More accurate information about E_0 can be obtained from the temperature dependence of the PL linewidth shown in Fig. 1(b), particularly from the temperature T_2, which corresponds to the maximum of the PL linewidth. These characteristic temperatures are 50, 60, and 70 K for annealed, as-grown, and hydrogenated samples, respectively. Applying the previously established relation, one obtains a DOS energy scale of 4, 5, and 6 meV, respectively. This result agrees with the estimate based on the transient temperature T_{tr} and it also fits into the range of typical E_0 values for (GaIn)(NAs) QWs with low nitrogen content (see in Ref. [13, Table 3]).

Now we turn to the determination of the density of localized states N_0 in Eq. (1). The PL linewidth at T_2 and the absolute value of the Stokes shift are in particular sensitive to the value of N_0. Reduction of the Stokes shift along with the reduction of the PL linewidth at T_2 in Fig. 1(b) for the hydrogenated sample as compared to the as-grown and annealed samples indicates a reduction of the

density of localized states due to hydrogenation. One can quantify this effect using the ratio $\text{FWHM}(T_2)/\text{FWHM}(0)$ [13]. In our case this ratio is about 1.7 for both as-grown and annealed samples, and it is about 1.3 for the hydrogenated sample yielding the values $N_0\alpha^2 \approx 0.2$ and $N_0\alpha^2 \approx 0.1$, respectively. Assuming a localization length $\alpha \approx 28\,\text{Å}$ (see Section 4), we obtain the two-dimensional density of localized states in the as-grown sample as $N_0 \approx 3 \times 10^{12}\,\text{cm}^{-2}$.

3. Nonradiative recombination

So far we have considered an idealized model, in which all excited electron–hole pairs contribute to the PL spectrum even at high temperatures. However, the experimental data for dilute nitride semiconductors show evidence that the integrated PL intensity decreases by several orders of magnitude with increasing temperature [3,21].

Strong quenching of the PL intensity with increasing temperature suggests an activated character of nonradiative processes. In order to explain this phenomenon, Williams and Eyring [22] proposed a general model, where charge carriers tunnel through an energy barrier prior to their nonradiative recombination. According to that model, the temperature dependence of the PL in the case of i nonradiative channels follows [22]:

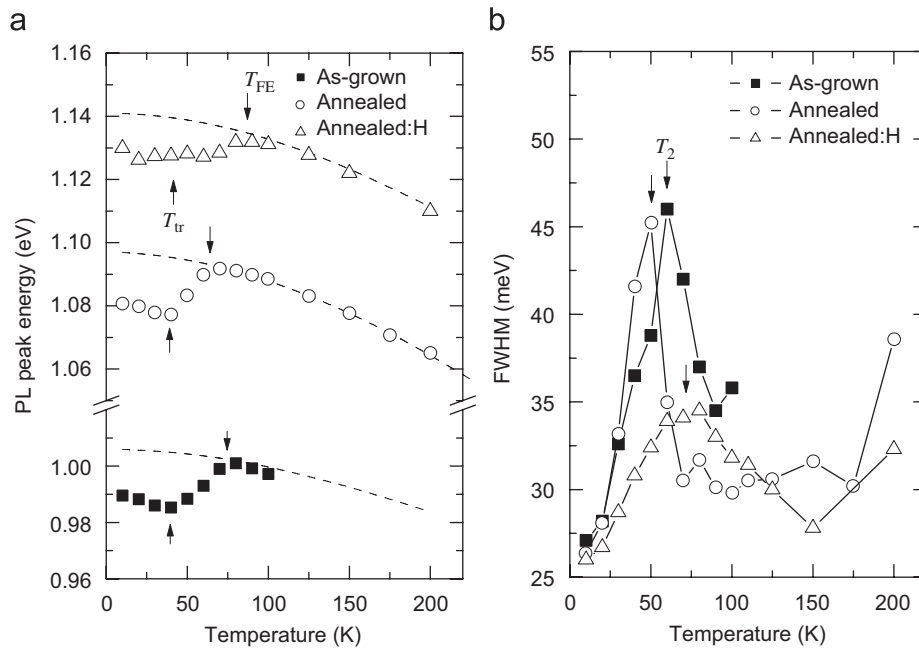$$I(T) = I_0 \left[1 + \sum_i A_i \exp(-E_i/k_B T) \right]^{-1}, \qquad (2)$$

Fig. 1. Experimental results for the PL peak position (a) and for the PL linewidth (b) as a function of temperature for $Ga_{0.7}In_{0.3}N_{0.006}As_{0.994}$/GaAs QWs after various postgrowth treatments. The measurements were performed using the low excitation intensity (12 mW). The dashed curves on panel (a) show the temperature variation of the PL peak energy measured with the high pump intensity (100 mW). The solid lines on panel (b) are guides to the eye. (After Hantke [31] and Hantke et al. [32].)

where E_i are the heights of the energy barriers, A_i are constants which are proportional to the transition probabilities between radiative and metastable states, and I_0 is the PL intensity at $T = 0$. The interpretation of the parameters in Eq. (2) depends on the particular experimental situation. For instance, in case of excitons bound to shallow defects, the activation energies E_i are associated with the exciton binding energy and with a dissociation energy of the bound exciton [23]. In case of heterostructures with shallow quantized states, the activation energies E_i are attributed to the energy differences between extended states in the barrier and quantized states in the QWs [24].

Eq. (2) is also popular in the dilute nitride semiconductor community, however, there is no general interpretation for the E_i energies. Some researchers interpret them as the energy separation between the conduction band edge and nitrogen-related localized states in the band gap [25]. Others associate different E_i energies with the energy separations between electron (or hole) subband levels [26]. Although Eq. (2) provides an excellent fit to the experimental data for temperature quenching of the PL in dilute nitride semiconductors, the assumption regarding the discrete energy states requires a better justification.

A generalized model for PL in disordered semiconductors has recently been suggested [16]. In this model, the empirical distribution of the energy barriers is replaced by an exponential DOS in the band tail [Eq. (1)]. In addition, a possibility of dynamic redistribution of carriers between radiative states in the band tail is taken into account, as it was done by Baranovskii et al. [11]. As a result, an excellent agreement between experimental data and theory was established (see Fig. 2). A comparison between the experimental data and results of the computer simulation provides important information on material parameters, such as the ratio between concentrations of nonradiative centers and traps $N_{nr}/(N_{nr} + N_0)$ and the disorder energy scale E_0. It is remarkable that the obtained value $E_0 = 8\,\text{meV}$ for (GaIn)(NAs) QWs agrees with the value $E_0 \approx 5\,\text{meV}$ deduced from the temperature-dependent PL measurements (see Section 2).

In order to perform a faster analysis of experimental data, an alternative simplified analytical model of the temperature quenching of PL was suggested [16,27]. The model is formulated on the basis of that proposed by Gee and Kastner [28], assuming that an exciton thermally activated to the mobility edge does not necessarily recombine nonradiatively, but can be recaptured into a radiative state with probability $N_0/(N_{nr} + N_0)$. A simplification is introduced at the expense of neglecting the energy relaxation of recombining carriers prior to recombination events. The principal difference between these two models—analytical model and kinetic Monte Carlo simulation—becomes apparent at low temperatures. At low temperatures, excitons trapped into localized states perform energy-loss hopping transitions between

the traps. Concomitantly, the energy distribution of excitons shifts towards deeper states in the band tail with respect to the mobility edge. Hence, the activated nonradiative recombination becomes weaker as compared to that given by the analytical model, in which it was implicitly assumed that excitations are frozen after the first capture event and no dynamical exchange between traps is allowed.

The agreement between the analytical theory and results of the computer simulation is established at high temperatures ($T \gtrsim E_0/k_B$), when thermal release to the mobility edge becomes efficient and intersite dynamics does not play an essential role anymore. In this temperature range, the PL intensity approaches its asymptotic value $I/I_0 \approx [1 + N_{nr}v_0\tau_0/(N_{nr} + N_0)]^{-1}$ (see Fig. 2), where v_0 is the attempt-to-escape frequency, which is usually assumed to be of the order $10^{13}\,\text{s}^{-1}$. We would like to emphasize that the level of the high-temperature plateau in the $I(T)$ dependence provides a straightforward estimate for the combination
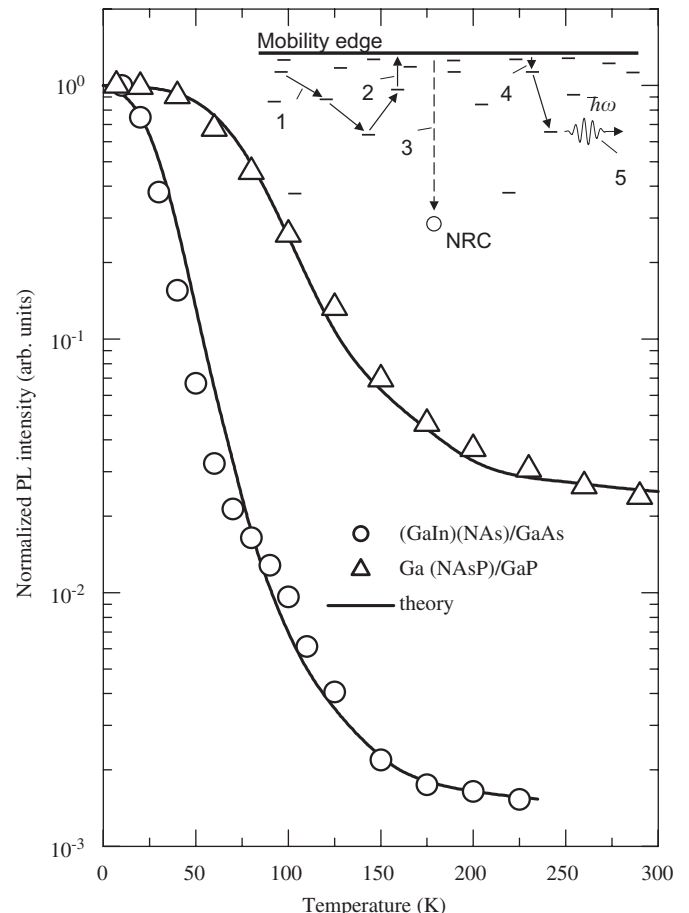

Fig. 2. Experimental data for the normalized PL intensity (I/I_0) as a function of temperature for $Ga_{0.7}In_{0.3}N_{0.006}As_{0.994}/GaAs$ and $GaN_{0.04}As_{0.80}P_{0.16}/GaP$ QWs (symbols). Solid lines show the results of the kinetic Monte Carlo simulation obtained with the following parameters: $\varepsilon_0 = 8\,\text{meV}$, $N_0\alpha^2 = 0.1$, $v_0\tau_0 = 10^4$, and $N_{nr}/(N_{nr} + N_0) = 0.12$ in case of (GaIn)(NAs) QWs, and $\varepsilon_0 = 10\,\text{meV}$, $N_0\alpha^2 = 0.01$, $v_0\tau_0 = 5 \times 10^4$, and $N_{nr}/(N_{nr} + N_0) = 1.4 \times 10^{-3}$ in case of Ga(NAsP) QWs. The insert illustrates schematically kinetic processes involved into the modelling. (After Rubel et al. [16].)

of material parameters $N_{nr}v_0\tau_0/(N_{nr} + N_0)$. An example for application of the simplified analytical theory to experimental data for temperature quenching of the PL in (GaIn)(NAs) QWs can be found elsewhere [27].

4. Nonexcitonic recombination

In existing theoretical studies of the dynamics of optical excitations in a disordered environment, one usually assumes that electrons and holes are spatially correlated in the form of excitons [11–14,16,19]. This assumption, however, is not always valid. For example, if the amplitude of the disorder potential or the temperature are larger than the binding energy of excitons, the assumption of strong spatial correlation between electrons and holes cannot be justified. This requires the consideration of dynamics and recombination of electrons and holes separately from each other. Additional information about these processes can be obtained from ultrashort time-resolved PL measurements.

The time-dependent luminescence spectrum provided by uncorrelated electrons and holes can be calculated as a convolution of the energy- and time-dependent carrier densities:[2]

$$I(\hbar\omega, t) \propto \int dE n^{(e)}(\hbar\omega + E, t)n^{(h)}(E, t), \qquad (3)$$

where $n^{(e)}(E, t)$ and $n^{(h)}(E, t)$ denote the densities of electrons and holes, respectively. Finding the $n(E, t)$ distribution is a complex problem, which could hardly be treated by computer simulations, in contrast to the case of excitons [11]. An efficient way to resolve the problem is to use rate equations for the carrier dynamics [29]. The rate equations describe the time evolution of the carrier density taking into account the hopping redistribution of electrons and holes between localized states, as well as their recombination.

Recombination of spatially separated electrons and holes occurs via their tunnelling across the intersite distance R. Analyzing the distribution of R's, one can show that the most efficient recombination takes place between localized states in which the states for electron and hole are separated by a distance, which is about the localization length α [30]. The recombination time of such pairs does not contain the exponential factor $\exp(-R/\alpha)$, and it is close to τ_0. Hence the recombination rate has the form [30]

$$v_r(t) \approx \tau_0^{-1}n(t)\alpha^2, \qquad (4)$$

where the product $n(t)\alpha^2$ takes into account a time evolution for the probability of finding these pairs. Under such circumstances, the recombination time is not a constant, in contrast to the exciton picture, and it is determined by the overall carrier density, which is itself a function of time. The time evolution of the carrier density is described by $dn/dt = -n(t)v_r(t)$, which gives rise to a
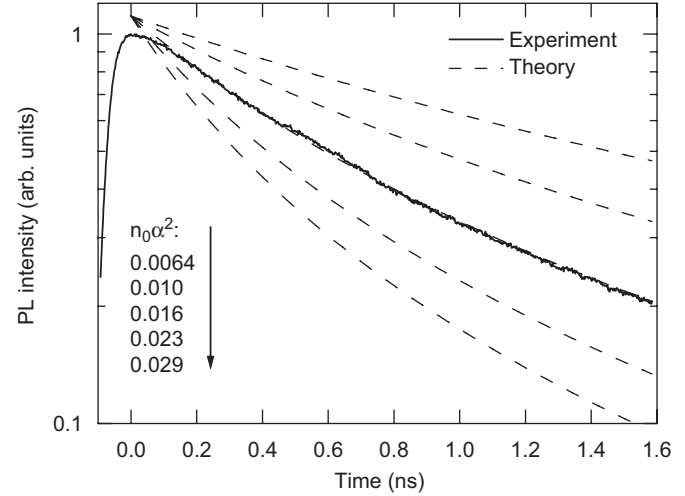

Fig. 3. Time evolution of integral PL intensity after a short pulse excitation of $Ga_{0.7}In_{0.3}N_{0.005}As_{0.995}$ multi QWs (solid line). Theoretical results obtained from Eq. (5) are shown by dashed lines for different $n_0\alpha^2$ values assuming $\tau_0 = 20$ ps. The agreement with experiment is obtained for $n_0\alpha^2 = 0.016$. (After Rubel et al. [29].)

time-dependence of the integrated PL intensity in the form

$$I(t) \propto \left(\frac{n_0\tau_0}{n_0\alpha^2 t + \tau_0}\right)^2, \qquad (5)$$

where n_0 is the density of electron–hole pairs generated right after the pulsed excitation. It is remarkable, that the PL spectrum depends on the particular choice of the DOS shape and temperature. However, the energy-integrated PL intensity is *not* sensitive to the DOS and temperature (provided we neglect nonradiative processes), since the recombination rate in Eq. (4) depends on the total carrier concentration, but not on its particular energy distribution [29].

The theoretical results for the integrated time-dependent PL intensity are compared with experimental data in Fig. 3. A notable feature of the time dependence of the PL intensity is its nonexponential character. Such a non-exponential behavior give evidence for a rather broad distribution of recombination times, which is difficult to bring into agreement with an exciton picture of the PL, since in the case of excitons the time decay would be a purely exponential function with a decay rate given by the lifetime of excitons [29]. The agreement between the theoretical results and experimental data is obtained for the magnitude of the parameter $n_0\alpha^2 = 0.016$. Taking into account an absorption coefficient in the QW, the estimate for the initial density of electron–hole pairs is about $n_0 \approx 2 \times 10^{11}$ cm^{-2}, which would lead to the estimate for the localization length of charge carriers $\alpha \approx 28$ Å [29].

5. Conclusions

Dilute nitride III–V semiconductor alloys possess a certain degree of disorder, which can be probed by

---

[2] Here we assume for simplicity, that the matrix element of the optical transition is independent of energy.

temperature- and time-dependent PL measurements. The results of the measurements, in particular, temperature dependences of the PL peak energy, of the PL linewidth, and of the integrated PL intensity, as well as a non-exponential time decay of the PL intensity in time-resolved PL measurements can be explained *quantitatively* in the framework of a model based on hopping and recombination of charge carriers in a manifold of localized states. The comparison between experimental data and the theory allows one to quantify disorder parameters. In particular, for the investigated (GaIn)(NAs)/GaAs QWs with nitrogen content below 1%, the energy spectrum of the localized states has an exponential form with the energy scale of $E_0 \approx 5$ meV and the concentration of localized states of $N_0 \approx 10^{12}$ cm^{-2} (assuming the localization length $\alpha \approx 28$ Å).

Acknowledgments

References

[1] M.-A. Pinault, E. Tournié, Appl. Phys. Lett. 78 (2001) 1562.
[2] I.A. Buyanova, W.M. Chen, G. Pozina, J.P. Bergman, B. Monemar, H.P. Xin, C.W. Tu, Appl. Phys. Lett. 75 (1999) 501.
[3] L. Grenouillet, C. Bru-Chevallier, G. Guillot, P. Gilet, P. Duvaut, C. Vannuffel, A. Million, A. Chenevas-Paule, Appl. Phys. Lett. 76 (2000) 2241.
[4] R. Kudrawiec, G. Sek, J. Misiewicz, L.H. Li, J.C. Harmand, Eur. Phys. J. Appl. Phys. 27 (2004) 313.
[5] T.H. Chen, Y.S. Huang, D.Y. Lin, K.K. Tiong, J. Appl. Phys. 96 (2004) 6298.
[6] A. Hierro, J.M. Ulloa, J.M. Chauveau, A. Trampert, M.A. Pinault, E. Tournié, A. Guzman, J.L. Sanchez-Rojas, E. Calleja, J. Appl. Phys. 94 (2003) 2319.
[7] M.S. Skolnick, P.R. Tapster, S.J. Bass, A.D. Pitt, N. Apsley, S.P. Aldred, Semicond. Sci. Technol. 1 (1986) 29.
[8] S.T. Davey, E.G. Scott, B. Wakefield, G.J. Davies, Semicond. Sci. Technol. 3 (1988) 365.
[9] E.M. Daly, T.J. Glynn, J.D. Lambkin, L. Considine, S. Walsh, Phys. Rev. B 52 (1995) 4696.
[10] R. Zimmermann, E. Runge, Phys. Stat. Sol. A 164 (1997) 511.
[11] S.D. Baranovskii, R. Eichmann, P. Thomas, Phys. Rev. B 58 (1998) 13081.
[12] H. Grüning, K. Kohary, S.D. Baranovskii, O. Rubel, P.J. Klar, A. Ramakrishnan, G. Ebbinghaus, P. Thomas, W. Heimbrodt, W. Stolz, W. Rühle, Phys. Stat. Sol. C 1 (2004) 109.
[13] O. Rubel, M. Galluppi, S.D. Baranovskii, K. Volz, L. Geelhaar, H. Riechert, P. Thomas, W. Stolz, J. Appl. Phys. 98 (2005) 063518.
[14] B. Dal Don, K. Kohary, E. Tsitsishvili, H. Kalt, S.D. Baranovskii, P. Thomas, Phys. Rev. B 69 (2004) 045318.
[15] K. Kazlauskas, G. Tamulaitis, P. Pobedinskas, A. Zukauskas, M. Springis, C. Huang, Y. Cheng, C.C. Yang, Phys. Rev. B 71 (2005) 085306.
[16] O. Rubel, S.D. Baranovskii, K. Hantke, B. Kunert, W.W. Rühle, P. Thomas, K. Volz, W. Stolz, Phys. Rev. B 73 (2006) 233201.
[17] P.R.C. Kent, A. Zunger, Phys. Rev. B 64 (2001) 115208.
[18] M. Galluppi, L. Geelhaar, H. Riechert, M. Hetterich, A. Grau, S. Birner, W. Stolz, Phys. Rev. B 72 (2005) 155324.
[19] S.D. Baranovskii, A.L. Efros, Sov. Phys. Semicond. 12 (1978) 1328.
[20] A. Miller, E. Abrahams, Phys. Rev. 120 (1960) 745.
[21] S. Shirakata, M. Kondow, T. Kitatani, Appl. Phys. Lett. 80 (2002) 2087.
[22] F.E. Williams, H. Eyring, J. Chem. Phys. 15 (1947) 289.
[23] D. Bimberg, M. Sondergeld, E. Grobe, Phys. Rev. B 4 (1971) 3451.
[24] G. Bacher, H. Schweizer, J. Kovac, A. Forchel, H. Nickel, W. Schlapp, R. Lösch, Phys. Rev. B 43 (1991) 9312.
[25] I.A. Buyanova, W.M. Chen, C.W. Tu, Solid-State Electron. 47 (2003) 467.
[26] R. Kudrawiec, M. Motyka, J. Misiewicz, H.B. Yuen, S.R. Bank, M.A. Wistey, H.P. Bae, J.S. Harris, J. Appl. Phys. 98 (2005) 063527.
[27] O. Rubel, S.D. Baranovskii, K. Hantke, W.W. Rühle, P. Thomas, K. Volz, W. Stolz, Phys. Stat. Sol. C 3 (2006) 2481.
[28] C.M. Gee, M. Kastner, Phys. Rev. Lett. 42 (1979) 1765.
[29] O. Rubel, S. Baranovskii, K. Hantke, J. Heber, J. Koch, P. Thomas, J. Marshall, W. Stolz, W. Rühle, J. Optoelectron. Adv. Mater. 7 (2005) 115.
[30] S.D. Baranovskii, B.I. Shklovskii, Sov. Phys. Semicond. 23 (1989) 88.
[31] K. Hantke, Ph.D. Thesis, Philipps-Universität Marburg, 2005.
[32] K. Hantke, J.D. Heber, S. Chatterjee, P.J. Klar, K. Volz, W. Stolz, W.W. Rühle, A. Polimeni, M. Capizzi, Appl. Phys. Lett. 87 (2005) 252111.